SCIENCE CHINA
Physics, Mechanics & Astronomy

• Article •

January 2015 Vol. 58 No. 1: 014301
doi: 10.1007/s11433-014-5526-x

Sound speed profile inversion using a horizontal line array in shallow water

LI ZhengLin[1,2*], HE Li[1], ZHANG RenHe[1], LI FengHua[1], YU YanXin[1] & LIN Peng[1]

[1] *State Key Laboratory of Acoustics, Institute of Acoustics, Chinese Academy of Sciences, Beijing 100190, China;*
[2] *Haikou Laboratory of Acoustics, Institute of Acoustics, Chinese Academy of Sciences, Haikou 570105, China*

Received September 7, 2013; accepted April 14, 2014; published online October 14, 2014

It is better to use a simple configuration to enhance the applicability of ocean environment inversion in shallow water. A matched-field inversion method based on a horizontal line array (HLA) is used to retrieve the variation of sound speed profile. The performance of the inversion method is verified in the South China Sea in June, 2010. An HLA laid at bottom was used to receive signals from a bottom-mounted transducer. Inverted mean sound speed profiles from 9-hour long acoustic signals are in good agreement with measurements from two temperature chains at the sites of the source and receiver. The results show that an HLA can be used to monitor the variability of shallow-water sound speed profile.

acoustic inversion, matched-field processing, horizontal line array

PACS number(s): 43.30.Pc, 43.30.Zk, 43.30.Re

Citation: Li Z L, He L, Zhang R H, et al. Sound speed profile inversion using a horizontal line array in shal-low water. Sci China-Phys Mech Astron, 2015, 58: 014301, doi: 10.1007/s11433-014-5526-x

Sound propagation in the ocean is strongly influenced by the ocean environment. The sound field is sensitive to the sound velocity of the water column and seafloor. This implies that, for example, the sonar detection of a sound source in range and depth depends on the environmental knowledge of a given propagation scenario. Conversely, the interaction between sound waves and the environment allows for retrieving environmental information from the acoustic signals. Munk and Wunsch [1] have introduced a ray-theoretic modeling named as Ocean Acoustic Tomography (OAT) to monitor the sea environment. OAT experiments in deep-water regions for large-scale ocean monitoring have used multiple sources and multiple arrays to determine the variability of the three-dimensional water temperature field [2–4]. This approach suffers degradation because of arrivals that cannot be identified or separated. An alternative approach, proposed by Munk et al. [5] and Shang [6], is modal tomography. This approach has some advantages over the traditional ray-theoretic approach, since the bottom and surface effects can be taken into account. Nevertheless, modal arrivals are not always identifiable. With the development of Matched-Field Processing (MFP) for source localization (see ref. [7] and references herein), Matched-Field Inversion (MFI) has been proposed to retrieve the ocean properties between source and receiver taking advantage of the spatial properties of the acoustic field and source location [8]. Several authors have used this technique for performing geo-acoustic inversions [9,10]. Tolstoy has applied MFI for sound speed profile (SSP) inversion and found that the acoustic fields propagate through a range-dependent series of sound speed profiles are identical to those propagating through simple range-independent environments given by the "averaged" sound speed profiles [11]. To avoid the complexity of the range-dependent environment, one can regard the environment as a range-independent one and invert its averaged sound speed profile

*Corresponding author (email: lzhl@mail.ioa.ac.cn)

directly.

In shallow water, the simple configuration with a single source and a single vertical array of receivers has been used in several occasions for inversion of SSP. The acoustic source is usually towed by a research vessel, to cover a certain area of interest, and the receiving array traditionally employed has a number of hydrophones to sufficiently sample higher order normal modes and assure as much as possible uniqueness in the problem solution [10]. A number of papers using sparse vertical arrays exist. Siderius et al. [12] used 4-hydrophone arrays distributed over a range of 40 km to invert range-dependent bottom properties from broadband transmission loss in the frequency band from 200 to 800 Hz. Felisberto et al. [13] demonstrated with experimental data that successful inversions for the water column in shallow water can be obtained with a 4-hydrophone vertical array using a known broadband source with a bandwidth of 700 Hz about 10 km away from the vertical array. Soares et al. have obtained inversion results using sparse vertical line arrays with four elements [14] and with three elements [15].

In China, the vertical line array has been used in SSP inversion successfully [16,17]. Current developments of receiver systems go in the sense of reducing the deployment requirements and increasing the safety. A horizontal line array (HLA) should be used in a shore-based sonar system. When a shore-based sonar system works, concurrent SSP is needed. It might be an alternative method to get the mean SSP from the acoustic signal for a shore-based sonar application. Using the pulse signals, Li et al. [18] has demonstrated the feasibility of SSP inversion from an HLA in the Yellow Sea. Howerer, the experimental configuration was not for SSP inversion. Only several SSPs and signals were measured during the experiment. It is worthy to design a special experiment for SSP inversion tests using an HLA and repeated acoustic signals from a transducer.

1 Experiment description

The experiment was conducted in the South China Sea in June 2010. One of the primary goals of the experiment was to study the feasibility of acoustic inversion for SSP with an HLA. The signals were emitted from a bottom-mounted source and received by a 70-element HLA with total length of 210 m as shown in Figure 1. The relative sites of the source and HLA are fixed, and the source is in the direction of 60° and at a range of 40 km from the center of the HLA. The source depth is 8 m above the sea floor. Water depth along the source receiver path is relatively flat with a mean depth of 98.5 m. The linear frequency module (LFM) signals from 120 Hz to 250 Hz with a duration of 1 s were continuously emitted six times every minute. The nominal maximum source level at the transducer resonance (about 180 Hz) was 175 dB *re* 1 μPa @ 1 m. The original six repeated LFM signals from the transducer is denoted as $s(t)$. The received signal from one element of HLA can be expressed as:

$$s_R(t) = \int S(\omega)P(r,z;\omega)\exp(-\mathrm{i}\omega t)\mathrm{d}\omega, \tag{1}$$

where $S(\omega)$ is the spectrum of $s(t)$, and $P(r, z; \omega)$ is the transfer function of the ocean environment from source to receiver. Pulse compression technique, which correlates $s(t)$ with $s_R(t)$, is used to increase the signal-noise-ratio (SNR). The compressed signal can be expressed as:

$$S_C(t) = \int |S(\omega)|^2 \, p(r,z;\omega)\exp(-\mathrm{i}\omega t)\mathrm{d}\omega. \tag{2}$$

In fact, $S_C(t)$ is the received signal of the self-correlation function of $S(t)$ propagating through the ocean channel $p(r, z; \omega)$.

Figure 2(a) gives the received original signals. LFM signals are submersed by the large amplitude airgun signals at a 10-s interval from a nearby oil exploration ship. Figure 2(b) gives signals after pulse compression with 6-s replica signal and Figure 2(c) is the first signal in Figure 2(b). It

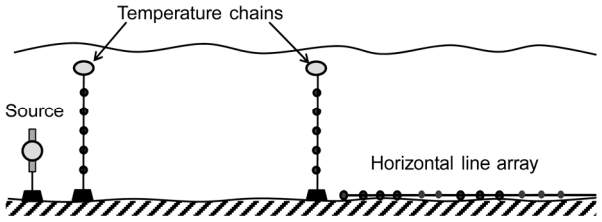

Figure 1 Experiment configuration.

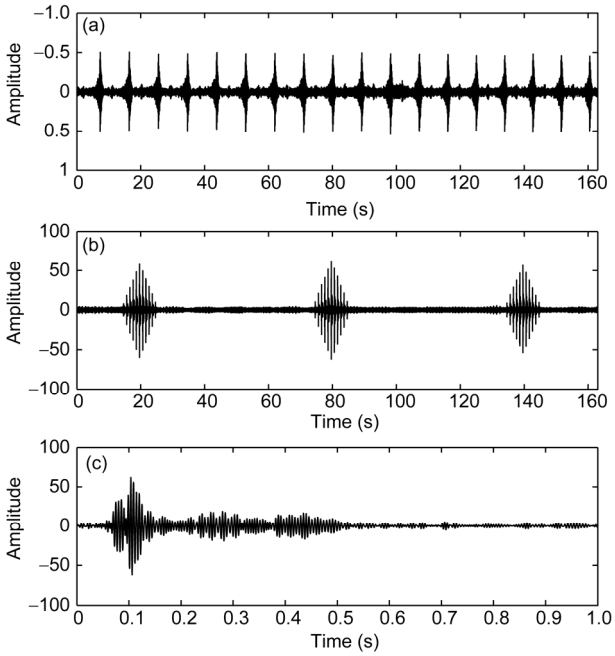

Figure 2 Received signals from one channel: (a) original signals, (b) received LFM signals after pulse compress, and (c) the first LFM signal shown in (b).

can be seen that the signal-noise-ratio (SNR) is greatly improved after signal compression. Two oceanography moorings with temperature depth sensors were deployed at both the source and the receiver sites, respectively, to monitor the thermocline variation of water column. Measured temperature profiles at different times are shown in Figure 3. The start time is 22:30 (GMT), June 7, 2010. There is a large period of time in which the LFM signals are greatly interfered by other noise sources. The white lines in Figure 3 indicate the time periods of acoustic signals with relatively high SNR. In comparison with Figure 2(b), Figure 4 gives a period of LFM signals with lower SNR. The LFM signals are greatly interfered by the unknown noise. Therefore, the signals with higher SNR as indicated in the time periods of Figure 3 are used in inversion. The spectrums of the signals in these periods are shown in Figure 5. One can see that the frequency spectrums of the signals at the duration of 9 hours varied with time. This variation was caused by the fluctuation of ocean SSP. A sensitivity study of thermocline depths on sound field is carried out. The sound field on HLA for SSPs with different thermocline depths are calculated and shown in Figure 6. The frequency space distributions of the sound field are different for the thermocline depths with 5-m variation. The results indicate that the SSP variation cause spectrum differences at different times. The main reason for the spectrum variation is that the fluctuation of the thermocline depth causes the arrival time to differ for normal modes [19]. Some lower modes with small grazing angle mainly propagate below the thermocline and their arrival times are relatively stable. Arrival time of some higher modes with larger grazing angle fluctuate with the thermocline depth. Therefore, the frequency spectrum for the three SSPs are different in Figure 6. It is why the acoustic signal from the HLA can be used for SSP inversion.

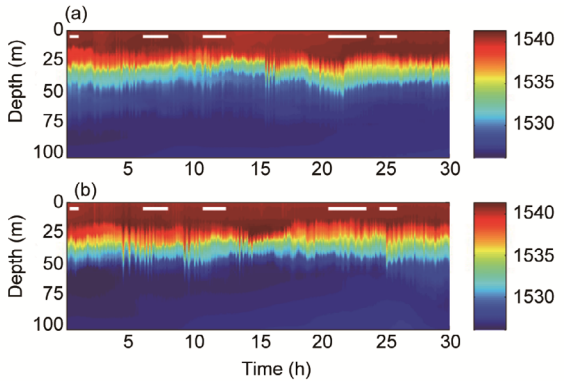

Figure 3 The sound speed profiles measured from two temperature chains. SSPs at (a) source site and (b) receiver site. The start time was 22:30 (GMT), June 7, 2010 and the white lines indicate the time period with higher SNR.

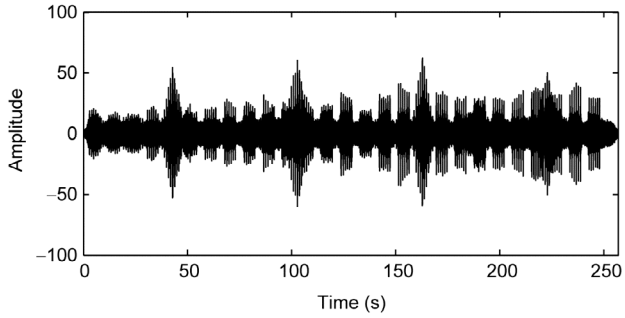

Figure 4 An example of the signals with lower SNR, in which the pulse compress has been done to increase SNR.

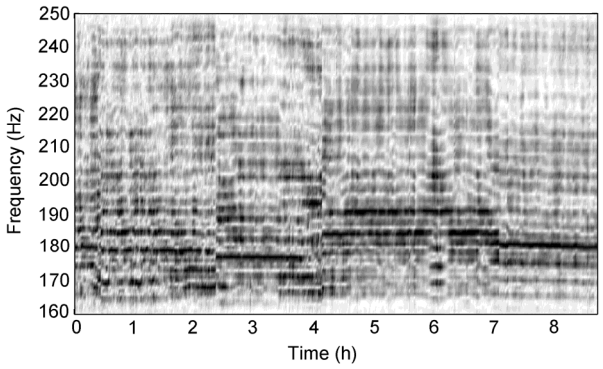

Figure 5 The spectrum of the signals with higher SNR at the time periods shown in Figure 3.

2 Inversion methods and inversion results

2.1 Sound speed profile reconstruction with empirical orthogonal functions (EOFs)

In MFI, the unknown parameters should be as few as possible to reduce the inversion uncertainty. LeBlanc proved that EOFs are a good function group for describing SSP [8]. Therefore, representation of SSP with a sum of EOFs can reduce the unknown parameters, and only the coefficients of EOFs need to be inverted. In our case, since a full set of observations are readily available, the EOF method is used for parameterization of SSP. Note that a similar expansion could be done using the temperature data as long as the salinity profile is known and is assumed to be constant through time. The EOFs are obtained using singular value decomposition (SVD) of a data matrix $\boldsymbol{C}$ with columns:

$$\underline{C}_i = c_i - \overline{c}, \tag{3}$$

where c_i are all available profiles, and $\overline{c}$ is the average profile. The SVD is known to be

$$\boldsymbol{C}=\boldsymbol{UDV}, \tag{4}$$

where $\boldsymbol{D}$ is a diagonal matrix with the singular values and $\boldsymbol{U}$ is a matrix with orthogonal columns, both of which are used as the EOFs. The SSP is obtained by

$$\underline{C}_{EOF} = \overline{c} + \sum_{n=1}^{n=N} \alpha_n \underline{U}_n, \tag{5}$$

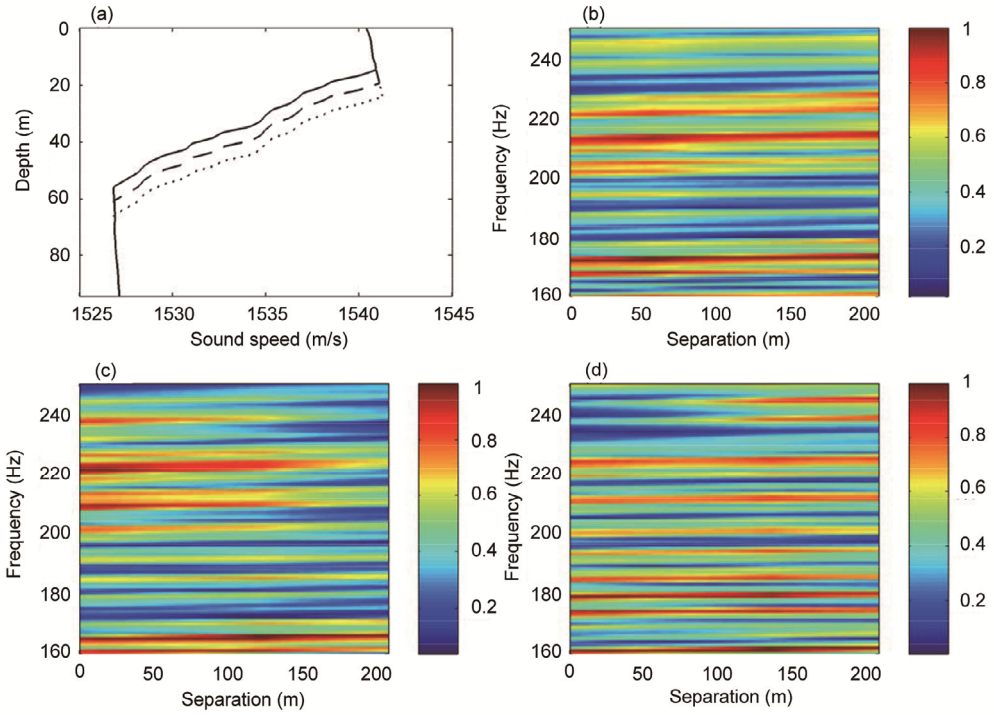

Figure 6 Sensitivity analysis of the thermocline depth on the sound fields of HLA, where the source receiver range is 40 km. (a) The sound speed profiles with different thermocline depths (without shifting, shifted by 5 m and shifted by 10 m); (b) the normalized spectrum on the HLA from the SSP without shifting (solid line); (c) the normalized spectrum on the HLA from the SSP on shifting by 5 m (dashed line); (d) the normalized spectrum on the HLA from the SSP on shifting 10 m (dotted line).

where N is the number of EOFs to be combined, which is judged by the accuracy of the representation of the SSP. Generally, a criteria based on the total energy contained on the first N EOFs is used. Experimental results have shown that usually the first two or three EOFs are enough to achieve the accuracy. The use of EOFs involves historical data that in the case of the water column SSP can be acquired over time and space. Thus, one can expect to have sufficient information to enable the model to obtain a profile that best represents the water column over range, depth, and time space. The SSPs obtained from the CTD measurements served as a database for estimation of the EOFs. The criteria used to select the number of relevant EOFs for the available data was

$$\widehat{N} = \min_{N}\left\{\frac{\sum_{n=1}^{N}\lambda_n^2}{\sum_{m=1}^{M}\lambda_m^2} > 0.8\right\}, \tag{6}$$

where the λ_n are the singular values obtained by the SVD, provided that $\lambda_1 \geqslant \lambda_2 \geqslant \cdots \geqslant \lambda_M$, where M is the total number of singular values. The coefficients α_n, which are the coefficients of the linear combination of EOFs, are unknown parameters and determined by matching between the measured acoustic data and the modeled data.

All SSPs shown in Figure 4 are used to extract the EOFs. Figure 7 summarizes the EOF analysis for the SSP measurements. Figure 7(a) shows the ensemble of the SSP (gray lines) and the average SSP (black line). Figure 7(b) shows the variations of residual SSPs. Figure 7(c) shows the percentage of total fit energy within the first 15 EOFs and Figure 7(d) shows the shape of the first six EOFs. It is shown that the first three EOFs contain approximately 90% of the energy. For this data set criteria, eq. (6) yields $\widehat{N} = 3$, that is, the first three EOFs are sufficient to model the sound speed with enough accuracy. Therefore, the coefficients of the first three EOFs are inverted in this paper.

2.2 The scheme of acoustic inversion

The SSP inversion is also a global optimization problem. Figure 8 shows the whole process of SSP inversion. A set of optimized coefficients (α_0) for EOFs is searched to obtain the minimum cost function ϕ_{cost} [20]:

$$\varphi_{\cos t}(\boldsymbol{\alpha}) = 1 - \left|\sum_{p=1}^{N}\sum_{q=p+1}^{N}\sum_{j=1}^{J}\left(D_{pq}(f_j)M_{pq}^{*}(\boldsymbol{\alpha}, f_j)\right)\right|(K_N)^{-1}, \tag{7}$$

where $D_{\text{pq}}(f)$ is the normalized cross-spectrum of the measured signals at frequency f: $D_{pq}(f) = D_p(f)D_q^{*}(f) / |D_p(f)D_q(f)|$, where $D_p(f)$ is the complex field received from the p-th hydrophone. $M_{pq}(\boldsymbol{\alpha}, f)$ is the normalized cross-spectrum of the modeled signals at frequency f and has

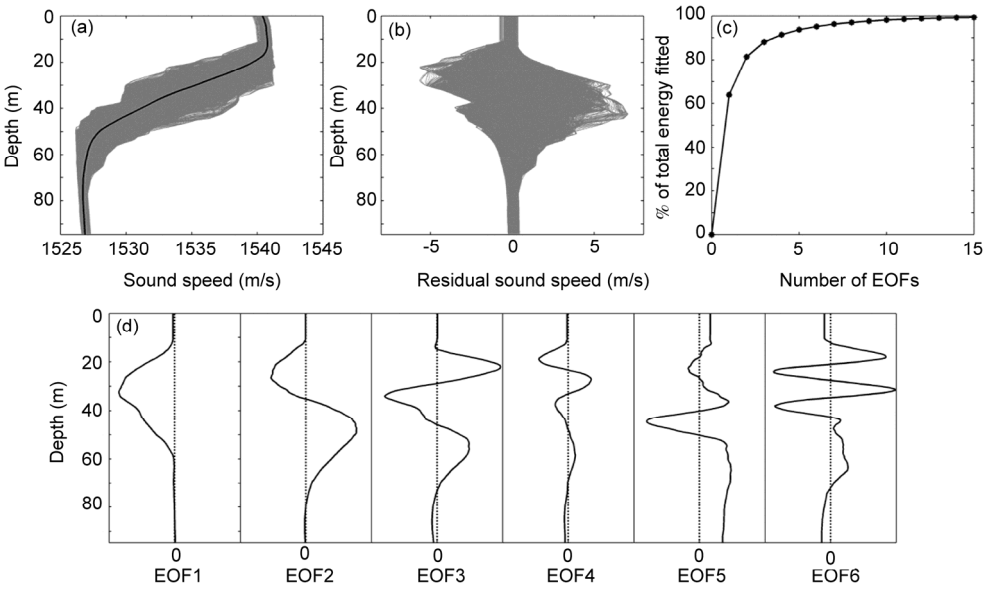

Figure 7 EOF analysis for the CTD casts. (a) Sound speed profiles and the averaged sound speed profile (thick line); (b) residual sound-speed profiles; (c) percent of total fit energy with limited sets of EOFs; (d) first six EOFs.

$$M_{pq}(\boldsymbol{\alpha}, f) = M_p(\boldsymbol{\alpha}, f) M_q^*(\boldsymbol{\alpha}, f) \Big/ \left| M_p(\boldsymbol{\alpha}, f) M_q(\boldsymbol{\alpha}, f) \right|,$$

where $M_p(\boldsymbol{\alpha}, f)$ is the complex pressure propagated from the source to the p-th hydrophone at frequency f with the environment $\boldsymbol{\alpha}$. N denotes the number of hydrophones and J is the points number of frequencies. "*" denotes the hetero conjugation and K_N is the normalized coefficient:

$$K_N = \left(\sum_{p=1}^{N} \sum_{q=p+1}^{N} \sum_{j=1}^{J} \left| D_{pq}(f_j)^2 \right| \right)^{1/2} \times \left(\sum_{p=1}^{N} \sum_{q=p+1}^{N} \sum_{j=1}^{J} \left| M_{pq}(\boldsymbol{\alpha}, f_j)^2 \right| \right)^{1/2}. \quad (8)$$

For the range-independent environment, the replica complex field $M_p(\boldsymbol{\alpha}, f)$ can be calculated from the normal mode theory [21]

$$P(r, z) = \frac{\mathrm{i} e^{-\mathrm{i}\pi/4}}{\rho(z_s)\sqrt{8\pi r}} \sum_m \psi_m(z_s)\psi_m(z) \frac{e^{\mathrm{i}k_{rm}r}}{\sqrt{k_{rm}}}, \quad (9)$$

where $\psi_m(z)$ is the m-th normal mode corresponding to horizontal complex wave number k_{rm}. The calculation of the modeled acoustic pressure fields are performed by the KRAKEN normal-mode acoustic propagation program.

Fitness evaluation of eq. (7), usually the most computationally demanding step, can be carried out independently for each individual environment coefficient α. A simple parallelized grid search technique, which divides the task of evaluating the population among several processors, is proposed to increase the inversion speed. By minimizing the misfit objective function of eq. (7), the most likely values of SSP can be estimated by substituting the optimized coefficients (α_0) into eq. (5).

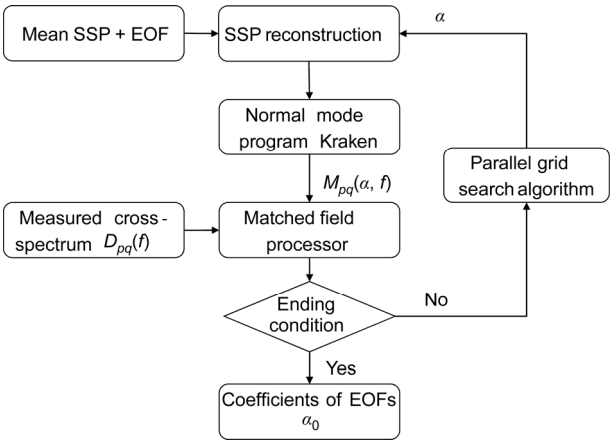

Figure 8 The flowchart of the MFP inversion for a HLA.

2.3 Inversion results

The SSP are assumed to be range-independent in the experimental region. With the empirical orthogonal functions, the first three orders of EOF coefficients could be used to reconstruct a SSP. The search bounds of the coefficients of the first three EOFs are listed in Table 1. They are taken from the maximal variation of EOF coefficients D in eq. (4). The acoustic signals shown in Figure 5 are used to invert for the SSPs. The frequency band used in MFI is from 175 Hz to 220 Hz with a frequency step of 1.0 Hz. A two layered

Table 1 Search bounds of the coefficients of the first three EOFs

Coefficient of EOFs	Lower bound	Upper bound
EOF1	–35	35
EOF2	–15	15
EOF3	–8	8

bottom model is used in inversion, which is inversed from the previously acoustic signals measured in March 2010 with a weak thermocline. The thickness of the sediment layer is 10 m. The sound speeds of the sediment layer and basement are 1585 m/s and 1650 m/s. The densities of the sediment and basement are 1.6 g/cm^3 and 1.8 g/cm^3, the attenuation coefficients of sediment and basement are 0.1 dB/λ and 0.3 dB/λ. The inversion results are shown in Figure 9, where Figure 9(a) gives the inverted SSPs, Figure 9 (b) is the mean SSPs from Figures 9(c) and 9(d), which are the SSPs measured at receiver site and the source site, respectively. It can be seen that the inversion results are comparable with the measured fluctuation of SSPs. Figure 10 give the comparison of the inversion results with the measured SSPs during the 21–24 h time period in Figure 4, where the solid lines are the inverted results, dashed line are the measured data, the number in the figure denotes the signal series number, and Δc gives the mean standard deviation error (STD). The STD of all results is shown in Figure 11(a), and the distribution of the STD is shown in Figure 11(b). It can be seen from Figures 10 and 11 that the inverted results are matched with the measured ones and the STD of most of the results less than 1 m/s. Therefore, it can be concluded that the acoustic data from HLA can estimate the mean SSP with relatively small error.

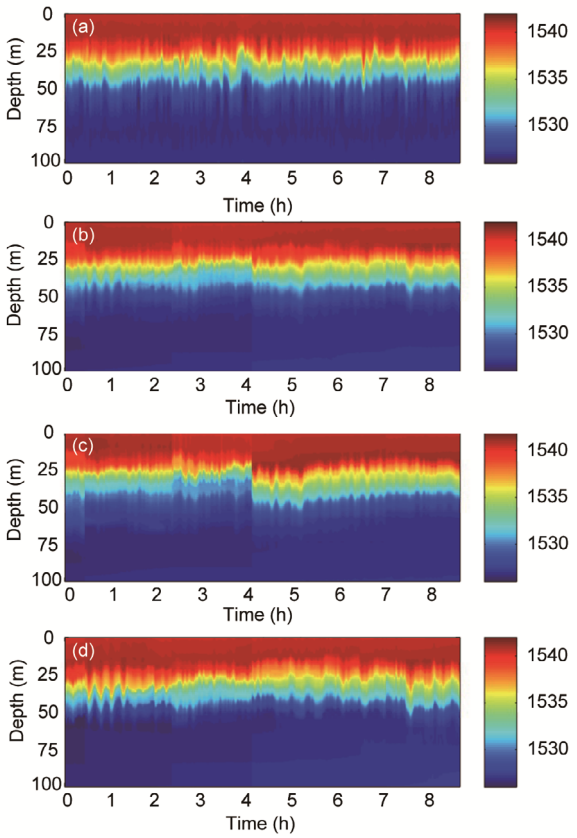

Figure 9 Comparison of the inversion results with the measured data: (a) inversion results from acoustic signals, (b) mean SSPs from the receiver site and source site, (c) measured SSPs at the receiver site, and (d) measured SSPs at the source site.

3 Conclusion

To enhance the applicability of SSP inversion in shallow

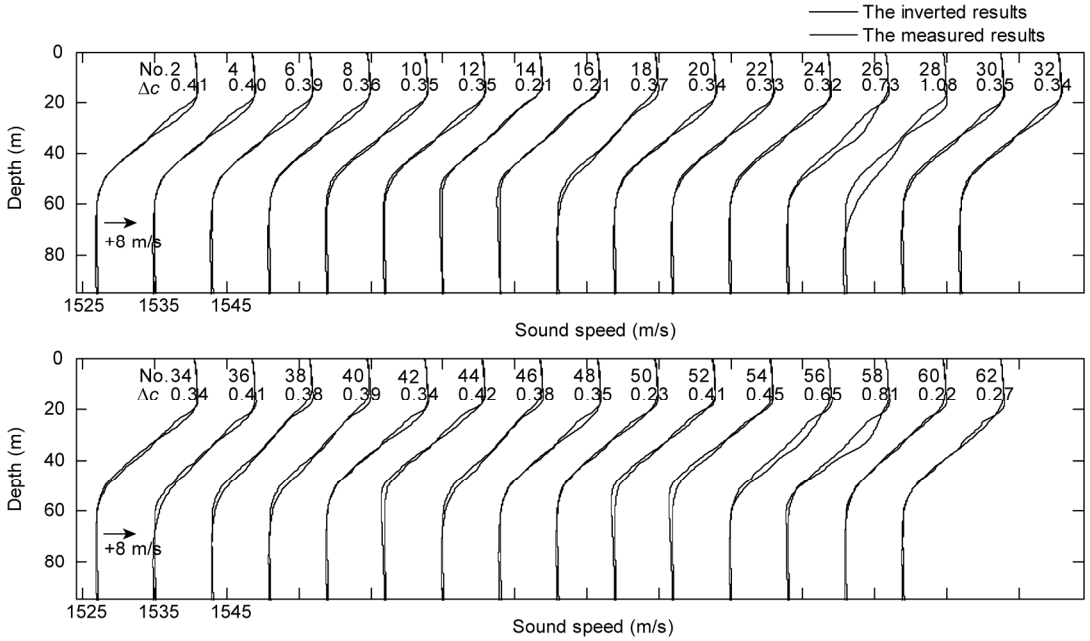

Figure 10 Comparison of the inversion results with the measured data for the time period 4.2–7.2 h in Figure 10, where the solid lines are the inversion results from the acoustic signals, the dotted lines are the measured SSPs at the receiver site.

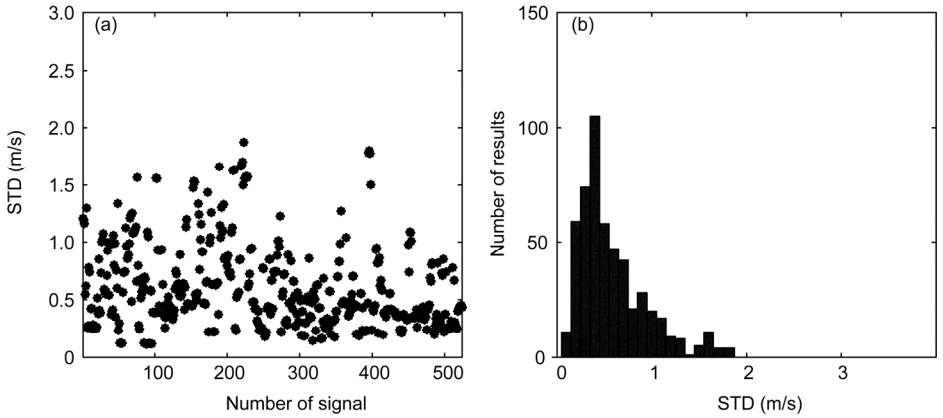

Figure 11 The STD error of inversion results (a) and distribution of STD (b).

water, a simple configuration of tomography consisted of HLA and a bottom-mounted source is proposed to retrieve the variation of water column. EOFs are used to represent the SSPs and reduce the unknown parameters, and the MFI method is used to invert for SSPs.

The performance of the HLA acoustic inversion is verified using the experiment data from South China Sea in June 2010. The mean SSPs at different times within a range of 40 km are inverted from the measured LFM acoustic signals. Nearly 9-hour long inversion results show the validity of the inversion scheme. It is the first special SSP inversion experiment in China. However, some issues remain to be investigated. For example, different groups of normal modes can be well excited if the source is located at different depths. Also, the group velocities of some modes at special frequencies are more sensitive to the thermocline depth variations. Therefore, additional work is needed to optimize the frequency band of the signal and the source depth according to the water depth.

The authors wish to express their thanks to the experimental team. This work was supported by the National Natural Science Foundation of China (Grant Nos. 11434012, 11404366, 11125420 and 11074269).

1 Munk W H, Wunsch C. Ocean acoustic tomography: A scheme for large scale monitoring. Deep Sea Res, 1979, 26(A): 123–161
2 Munk W H, Spindel R C, Baggeroer A B, et al. The heard island feasibility test. J Acoust Soc Am, 1994, 96: 2330–2342
3 Worcester P F, Spindel R C. North pacific acoustic laboratory. J Acoust Soc Am, 2005, 117: 1499–1510
4 Worcester P F, Munk W H, Spindel R C. Acoustic remote sensing of ocean gyres. Acoust Tod, 2005, 1(1): 11–17
5 Munk W H, Wunsch C. Ocean acoustic tomography: Rays and modes. Rev Geophys Space Phys, 1983, 21: 777–793
6 Shang E C. Ocean acoustic tomography based on adiabatic mode theory. J Acoust Soc Am, 1989, 85: 1531–1537
7 Baggeroer A B, Kuperman W A, Mikhalevsky P N. An overview of matched field methods in ocean acoustics. IEEE J Ocean Eng, 1993, 18: 401–424
8 Tolstoy A, Diachok O, Frazer N L. Acoustic tomography via matched field processing. J Acoust Soc Am, 1991, 89(3): 1119–1127
9 Gerstoft P, Gingras D. Parameter estimation using multi-frequency range dependent acoustic data in shallow water. J Acoust Soc Am, 1996, 99(5): 2839–2850
10 Snellen M, Simons D G, Siderius M, et al. An evaluation of the accuracy of shallow water matched field inversion results. J Acoust Soc Am, 2001, 109: 514–527
11 Tolstoy A, Diachok O, Frazer L N. Acoustic tomography via matched field processing. J Acoust Soc Am, 1991, 89(3): 1119–1127
12 Siderius M, Hermand J P. Yellow shark spring 1995: Inversion results from sparse broadband acoustic measurements over a highly range-dependent soft clay layer. J Acoust Soc Am, 1999, 106(2): 637–651
13 Felisberto P, Jesus S M, Stephan Y, et al. Shallow water tomography with a sparse array during the intimate'98 sea trial. In: MTS/IEEE, editor, Proceedings MTS/IEEE Oceans'2003, San Diego, USA, 2003. 571–575
14 Soares C, Jesus S M, Coelho E. Acoustic oceanographic buoy testing during the maritime rapid environmental assessment 2003 sea trial. Simons D, ed. In: Proc. of European Conference on Underwater Acoustics 2004, Delft, Netherlands, 2004. 271–279
15 Soares C, Jesus S M. Matched-field tomography using an acoustic oceanographic buoy. In: Jesus S M, ed, Proceedings of European Conference on Underwater Acoustics 2006, Carvoeiro, Portugal, 2006. 717–722
16 Yu Y X, Li Z L, He L. Matched-field inversion of sound speed profile in shallow water using a parallel genetic algorithm. Chin J Oceanol Limnol, 2010, 28(5): 1080–1085
17 He L, Li Z L, Zhang R H, et al. Inversion for sound speed profiles in the northern of South China Sea (in Chinese). Sci Sin-Phys Mech Astron, 2011, 41(1): 49–57
18 Li F H, Zhang R H. Inversion for sound speed profile by using a bottom mounted horizontal line array in shallow water. Chin Phys Lett, 2010, 27(8): 084303-1-4
19 Li Z L, Zhang R H, Badiey M, et al. Arrival time fluctuation of normal modes caused by solitary internal waves (in Chinese). Sci Sin-Phys Mech Astron, 2013, 43(1): s62–s67
20 Westwood E K. Broadband matched-field source localization. J Acoust Soc Am, 1992, 91: 2777–2798
21 Jensen F B, Kuperman W A, Porter M B, et al. Computational Ocean Acoustics. 2nd ed. New York: Springer, 2011